

Integration of Remote Sensing and Particle Tracking Modeling to Locate Marine Litter Accumulations in Manila Bay Pasig River Outfall

Fredrik Angelo F. Francisco¹, Erlyn Kaye P. Mortega¹, Ayin M. Tamondong¹, Eugene C. Herrera²

¹ Department of Geodetic Engineering, University of the Philippines, Diliman, Quezon City, Philippines - (fffrancisco, epmortega, amtamondong)@up.edu.ph

² Institute of Civil Engineering, University of the Philippines, Diliman, Quezon City, Philippines - echerrera1@up.edu.ph

Keywords: Plastic, Marine Litter, Marine Debris, Particle Tracking, Remote Sensing, Marine Pollution, Manila Bay

Abstract

Plastic pollution remains one of the world's most prevalent pollution problems, especially in the Philippines. The main objective of the study is to develop a methodology for locating marine litter accumulations between remote sensing images and a particle-tracking model beyond the sparse historical information and sources of Manila Bay Pasig River Outfall's plastic litter from 2017 to 2019. We aim to bridge the gap between the two technologies by using the earliest classified marine litter points as input sources for the particle-tracking model, then comparing other detections with the calculated positions from the model and a control simulation of marine litter particles from Pasig River's mouth. Marine litter was detected near coastal areas and in open waters, with 68% average accuracy. With a localized hydrodynamic model, the particle tracking model successfully simulated 188 remotely sensed plastic particles in both input approaches from 2017 to 2019. Marine litter positions showed higher correlation when using remote sensing sources as opposed to the riverine source of Pasig River, with average R-squared values from 0.91 and 0.92 to 0.95 and 0.96, respectively, in each axis; however, both approaches also showed high variance. In all results, we observed significant accumulation near the Manila Bay Port, particularly during the wet season. In summary, our study showed significant advantages in using remote sensing data in conjunction with particle tracking models in locating marine litter with high spatial and temporal resolution, and highly recommends coupling the technologies together for future studies.

1. Introduction

1.1 Background of the Study

Plastic pollution remains one of the world's most prevalent pollution problems. The Philippines is regarded as one of the world's leading and largest contributors to marine plastic pollution (Paler et al., 2022; Meijer et al., 2021). The country faces direct impacts from this growing issue which are especially evident in Manila Bay, where waste is discharged from 17 major rivers, including the Pasig River. Deteriorating water quality from land runoff and urban waste pollution, severe coastal erosion, and marine habitat degradation (Cruz & Shimozono, 2021) are some of the impacts seen in the bay.

Monitoring marine plastic litter is crucial for both preemptive and active waste management, as microplastic debris always poses significant risks to marine life and the environment (Cruz & Shimozono, 2021; Waqas et al., 2023). Some of the promising approaches are Lagrangian-based Particle Tracking Models (PTMs) and remote sensing which have been used to simulate and detect marine litter, independently. Each method has advantages but also limitations. PTMs often validate results using shoreline plastic accumulation data, which poorly represents actual interactions (Carlson et al., 2017), while remote sensing validation is limited by scarce and costly in-situ measurements (Waqas et al., 2023). From these limitations, we aimed to bridge the gap between the two methodologies to accommodate and answer each method's drawbacks.

1.2 Research Objectives and Significance

The main objective of the study is to develop a methodology for detecting and locating marine plastic litter accumulations using remote sensing data and a Lagrangian Particle-Tracking Model beyond the sparse historical data of Manila Bay's plastic litter

from 2017 to 2019. Aligned with the study's objective, the study specifically aims to:

1. Identify and map marine plastic litter accumulations from the Manila Bay Pasig River outfall using satellite images from Sentinel-2;
2. Simulate plastic pollution movement with Lagrangian PTM(s) in the Manila Bay Pasig River outfall and locate accumulations and endpoints;
3. Evaluate the spatial distribution and level of agreement of located marine plastic litter accumulations between the PTM and remote sensing results.

The study's purpose is aligned with two of the United Nations Sustainable Development Goals (SDG), specifically SDG 6 and SDG 14. This study supports SDG 6: Clean Water and Sanitation, specifically through target 6.3 by contributing to efforts to reduce water pollution and improve water quality. Similarly, this study also addresses the first target of SDG 14: Life Below Water to prevent and significantly reduce marine pollution of all kinds including marine plastics by 2025.

1.3 Scope and Limitations

The research was done only within a set area of observation, the Manila Bay Pasig River outfall, in both remote sensing and particle tracking from 2017 to 2019. With regards to the computationally intensive methods of particle-tracking, hydrodynamic modeling of the complete Manila Bay was not performed. It is important to note that wind input was not included in the hydrodynamic model due to the unavailability of wind data. This research focused specifically on marine debris as defined in the Marine Debris and Oil Spill (MADOS) dataset, which includes floating plastics and mixed anthropogenic debris (Kikaki et al., 2024). This definition closely aligns with the

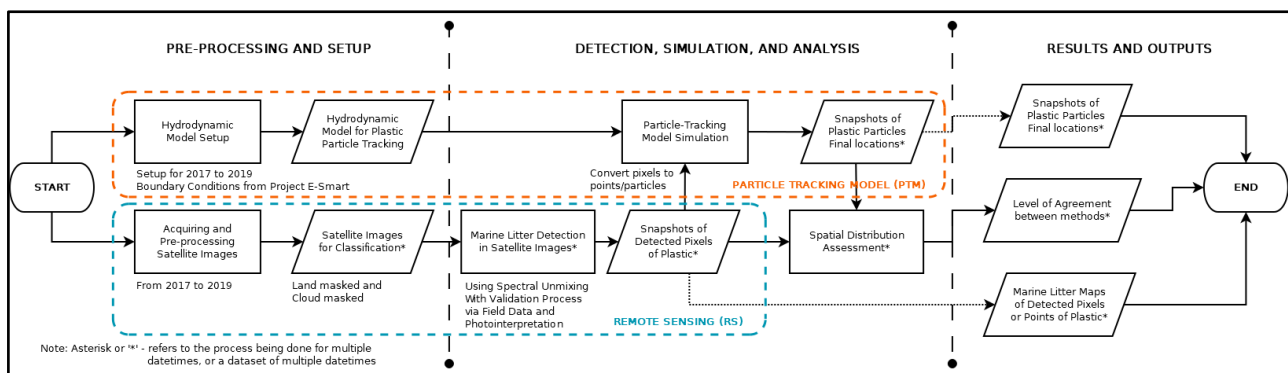


Figure 1. Detailed methodology flowchart

United Nations' broader definition of marine litter. For this study, marine litter and marine debris is used interchangeably to refer to marine litter. This assumption was made since plastics are the most abundant marine litter collected by the International Coastal Cleanup (ICC), the world's largest volunteer effort aimed at removing and collecting litter in water bodies. Other types of marine litter, such as submerged debris will not be considered due to detection limitations and the study's focus on floating debris observable from satellite imagery. Additionally, the detected marine litter's specific dimensions cannot be discerned due to the apparent nature of mixed pixels for marine debris. However, based on Sentinel-2's RGB spatial resolution, each classified pixel or tracked particle still corresponds to an area of no more than 100 square meters.

This research was experimental in nature. Had the results shown a strong match between the model simulations and the remote sensing outputs, additional simulations would have been conducted using scenarios with varying levels of plastic presence. These planned scenarios aimed to analyze current trends in plastic pollution around the Pasig River outfall in Manila Bay. However, suppose the results had shown a mismatch or negative agreement between the particle-tracking simulations and the detected marine litter. In that case, the study will shift its focus toward identifying the limitations of both approaches and the combined method. Possible solutions to these limits were explored and discussed within the same interdisciplinary framework, but the testing of solutions is suggested for future research.

2. Methodology

This study integrates remote sensing techniques with particle-tracking models to detect, locate, and analyze the spatial behavior of plastic pollution in Manila Bay Pasig River Outfall. Figure 1 shows the detailed overall process that we utilized to combine the two technologies, which will be further discussed in subsequent sections.

2.1 Study Area

As previously mentioned, this research will focus on the Manila Bay Pasig River outfall, highlighted in Figure 2, using remote sensing and particle tracking, with data from 2017 to 2019. In remote sensing, specifically in subsetting satellite images, the spatial extents were approximated from the spatial extents of the grid generated in Delft3D for the Particle Tracking Model, but slightly larger than the grid to ensure that all pixels within the resulting model's grid are processed. In the Particle Tracking Model, a grid was generated in Delft3D or RGFRID, with the

GADM administrative boundaries used as land boundaries as a visual reference. The generated grid's extents range from 120.761445 ° E to 121.015749 ° E in the E-W direction, and 14.446978 ° N to 14.691675 ° N in the N-S direction, as shown in Figure 3.

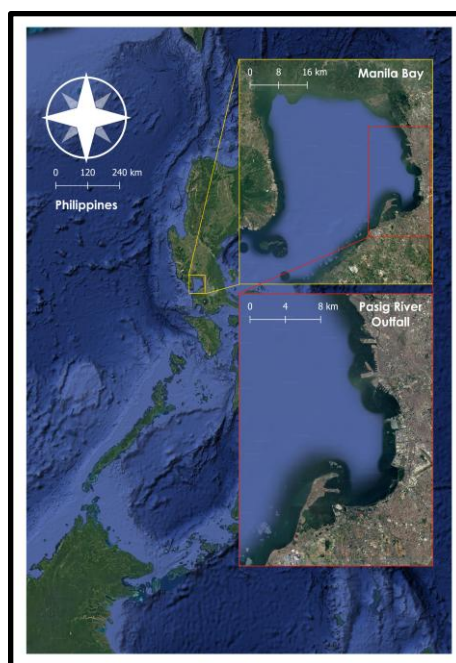


Figure 2. Study area.

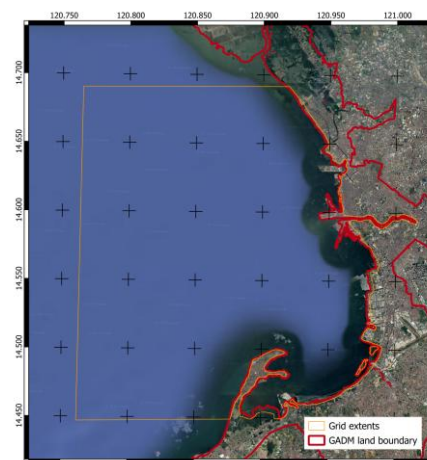


Figure 3. Generated Delft3D grid extents.

2.2 Marine Plastic Litter Detection

The multispectral optical satellite missions, Sentinel-2A and Sentinel-2B, from the European Space Agency (ESA), served as the primary data source for satellite imagery due to their relatively high spatial resolution, with certain bands offering a resolution of 10 meters. These satellites provide 13 available bands per image, spanning the Visible to Shortwave Infrared (SWIR) spectrum. A quality cloud mask for each image provided by Sentinel is also obtained. It is noted that in processing these images, not all bands are included due to the limitations of linear spectral unmixing and the significant difference in wavelength between bands. The actual bands used in processing only included Band 1 through Band 8A. The images used in this study are atmospherically corrected, specifically in the form of Level 2A images, which provide surface reflectance values. A total of 26 images were collected, with only the months with clear enough cloud cover for the study area. The method for classification used Spectral Unmixing with a fully constrained Linear Spectral Unmixing (LSU) Algorithm in the Sentinel Application Platform or SNAP.

$$R_k = \sum_i^n a_i \cdot E_{i,k} + \varepsilon_k \quad (1)$$

where R_k is the reflectance of source at wavelength k
 $E_{i,k}$ is the reflectance at endmember i at wavelength k
 ε_k is the abundance of endmember i
 n is the number of endmembers
 m is the number wavelengths in discrete spectrum

The spectral analyses of the results of the Marine Debris and Oil Spill or MADOS dataset from Kikaki et. al. (2024) were used in utilizing the spectral unmixing tools. In their holistic dataset, the 15 thematic classes were identified in marine environments. It is noted that we did not utilize all classes, due to the limits of the spectral unmixing tool. Of the 15 classes, the spectral analyses of marine debris, oil spill, marine water, natural organic material, sediment-laden water, shallow water, ship, turbid water, and waves & wakes were used. A plot of the spectral signature of each used thematic class can be seen in Figure 3. After running the linear spectral unmixing tool in SNAP, to complete classification, all pixels where marine debris abundance is greater than 0.50 or 50%, or in other words majority marine litter, are classified as marine plastic litter.

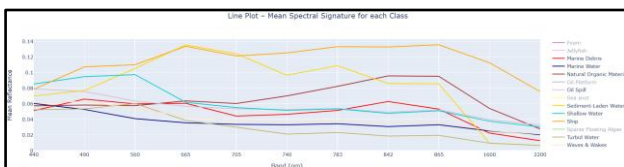


Figure 3. Spectral analyses of MADOS thematic classes (Kikaki et. al., 2024)

For validation, in selecting validation pixels, we were guided by the image interpretation key from the sample images of each MADOS class described on their website (Kikaki et. al., 2024). Additionally, relevant bands and indices, as shown in Table 1, were used for creating validation data through image and index interpretation. These indices were useful in creating false-color composites that further differentiate the thematic classes through simple visualization in SNAP.

Index	Decryption	Equation	Equation for Sentinel-2
FDI	Floating Debris Index	$RE2 + (SWIR1 - RE2) \times ((\lambda NIR - \lambda RED) / (\lambda SWIR1 - \lambda RED)) \times 10$	$B8 - (B6 + (B11 - B6)) \times ((\lambda B8 - \lambda B4) / (\lambda B11 - \lambda B4)) \times 10$
PI	Plastic Index	$NIR / (NIR + Red)$	$B8 / (B8 + B4)$
NDVI	Normalized Difference Vegetation Index	$(NIR - Red) / (NIR + Red)$	$(B8 - B4) / (B8 + B4)$
NDWI	Normalized Difference Water Index	$(Green - NIR) / (Green + NIR)$	$(B3 - B8) / (B3 + B8)$

Table 1. Indices for image interpretation (Danilov & Serdiukova, 2024)

2.3 Particle Tracking Model

A hydrodynamic model is necessary before particle tracking modeling in order to accurately model the study area's morphology and hydrodynamics. The hydrodynamic model was created and derived using Project e-smart's local model for Manila Bay and its open boundaries from 2017 to 2019 within the computational fluid dynamics software Delft3D. Project e-SMART's larger model was calibrated from January 2017 to December 2019, during which field measurements were compared and assessed with the model. According to Project e-SMART, the Manila Bay model includes Pasig River, Laguna Lake, and Manila Bay itself, where the size of the grid cells varies from 0.02 to 2 km (2021). In their model, they used 50 discharge points located at river outlets, initial salinity and temperature, and meteorological inputs derived from local weather stations. Using observation points and running the larger model from 2017 to 2019, the open boundary conditions necessary for establishing the study area's hydrodynamic model were obtained and synthesized. Figure 4 shows the observation points coinciding with the boundaries of our grid; however, to simplify the new model and simulations, only four observation points were recorded: N4, W6, S3, and the first Pasig River boundary point. Each point provided the water surface elevation (m); depth average, near surface, mid section, near bottom velocities (m/s); And depth average, near surface, mid section, near bottom discharges (m³/s). These values were synthesized and converted into time series boundary conditions for the hydrodynamic model. The model was then run with the appropriate domain information, such as bathymetry from GEBCO 2024, time frame, and uniform initial conditions at 0 water level.

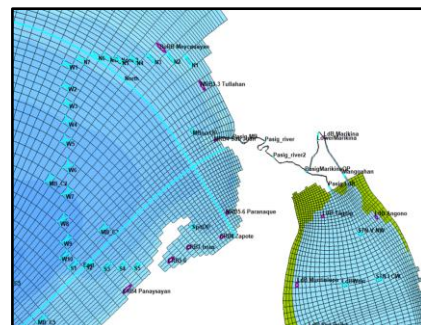


Figure 4. Observation points from Project e-SMART, coinciding with the study area grid

After running the hydrodynamic model, its hydrodynamics is used in Delft3D's Particle tracking module or Delft3D-PART. After classification and validation in Marine Plastic Litter Detection, the earliest classified image's pixels were used as the input for the PTM releases to observe the particle movement over time in tandem with the Remote Sensing Data. These pixels were also further aggregated into 1-kilometer clusters with the DBSCAN clustering tool in QGIS. Details like the mean center of each cluster and average marine debris abundance were also taken into account per cluster to be used as input information for each release. One instantaneous release is made per cluster, and their release positions or points can be seen in Figure 5.

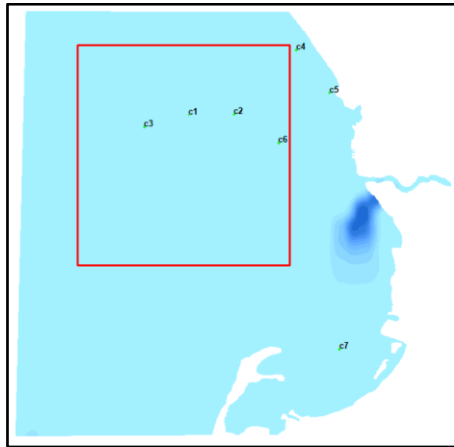


Figure 5. Instantaneous particle tracking model releases (c#) using remotely sensed input points with arbitrary zoom grid (Red)

As a control for comparison, we also ran the particle tracking model using the same hydrodynamic conditions but with a single instantaneous release as seen in Figure 6. In this setup, all cluster information was aggregated and released from only one location, the mouth of the Pasig River. This setup reflects the common assumption in many particle tracking studies, as seen in the literature (Cruz & Shimozone, 2021; Politikos et al., 2017), where marine litter begins from riverine mouths. It was used to compare with our approach, which utilizes remotely sensed data as input for source locations. After running the two simulations, we also took note of the number of particles within the domain for both simulations throughout the 3-year time frame to observe the exit of the particles to the rest of the bay.

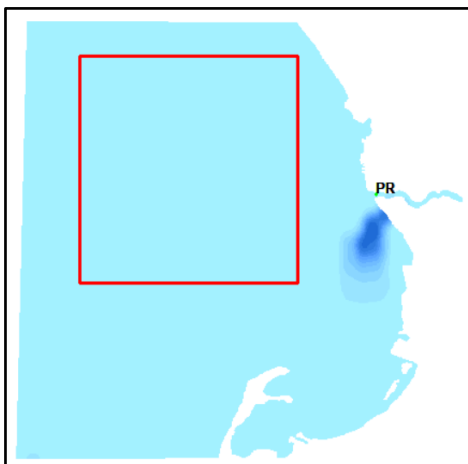


Figure 6. Instantaneous particle tracking model releases using riverine input points with arbitrary zoom grid (Red)

2.4 Spatial Distribution Assessment

To assess if the two methodologies of remote sensing and particle tracking coincide with each other, results from each methodology regarding their spatial distribution with each other were assessed through five different ways: (1) mapping spatial distribution by proximity, (2) generating a histogram of nearest point distances for all pairs of particles and pixels, (3) plotting XY Position Equal line scatter plots (or Line of Equality), (4) producing XY Position Bland-Altman Plots, and (5) creating XY Position Difference Plots.

2.4.1 Pixel-Pair Proximity Maps

Initially, once all outputs from the Marine Litter Detection and Particle Simulation have been generated, all classified image points and model snapshot particle positions will be compared through visualization in maps. These outputs have both been converted to vector points in QGIS. Conversion to points was done using the Centroids tool for each pixel or particle grid cell. This conversion was done for all matching datetimes. After conversion, both sets of points for a particular time step or datetime are ensured to have calculated attributes for ID, X position, and Y position in the Universal Transverse Mercator or UTM Zone 51N Cartesian coordinate system. Next, the two sets of points must be compared altogether for each time step. To quantify these comparisons, a proximity tool, Distance Matrix, will be employed for each pair of outputs to associate plastic particles with the corresponding classified pixels. Distance Matrix or Point Distance calculates the Euclidean distance between two points (ESRI, n.d.) and will be applied to all pixels and particles within each pair of outputs. An illustration from ESRI describing how the tool works is provided in Figure 7.

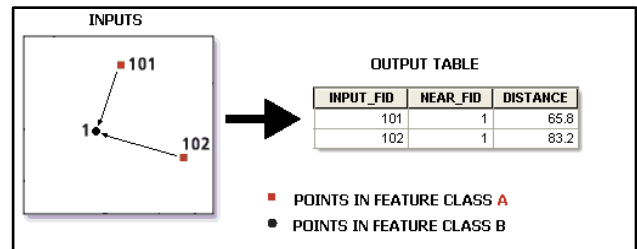


Figure 7. Distance matrix or point distance illustration (ESRI, n.d.)

This analysis operates under the assumption of a many-to-one relationship between particles and pixels, wherein one pixel can correspond to many particles, but each particle only corresponds to one pixel, the nearest to said particle. A many-to-one relationship was chosen due to multiple particles potentially accumulating on a single grid cell, hence, multiple particles may correspond to a single pixel, that pixel being the nearest pixel to the particles. All sets of points are mapped with their symbology representing the distance between each pair. This is done per datetime. For clarity, the same procedures are also done for the riverine control particles and remote sensing data.

2.4.2 Nearest Point Distance Histogram

With all measured distance values per pair of pixel and particle, a histogram is made to express the statistical distribution of the measured distances between the two methodologies. Through this Nearest Point Distance Histogram, we summarize the frequency distribution of distances into discrete bins for simpler statistical analysis and interpretation. We may also find other details regarding the differences in the two methods, such as the

skewing of the distribution and the most frequent distance measurements. Additionally, the mean, median, mode, and standard deviation of distances are also calculated. For clarity, the same calculations and histogram are also done for the riverine control particles and remote sensing data.

2.4.3 XY Position Equal-Line Plots

To compare the located positions between the two methods, a simple way is to treat each pair of points as supposedly equal in position. Therefore, an equal line scatter plot or line of equality plot is made by equating the pairs of X and Y coordinates with one another for all pairs of points per datetime. Other than the comparison with the line of equality, the plots' linear trendlines are also calculated and visualized in the plots. Furthermore, each plot's R-squared and linear regression equation are displayed for further analysis and interpretation. For clarity, the same procedures are also done for the riverine control particles and remote sensing data.

2.4.4 XY Bland-Altman Plots

Since position is a continuous value, Bland-Altman plots were used to compare the coordinate positions of plastic obtained from Remote Sensing and PTMs. For clarity, this procedure was only done for our approach and not the riverine control particles. Bland-Altman plots are best suited for estimating the agreement between two techniques on the same continuous variable, giving a graphical visualization of bias (Ranganathan & Aggarwal, 2017). For this study, the Bland-Altman plots are scatter plots of the difference between a pair of a pixel and a particle's position on a particular axis and the average of a pair of a pixel and a particle's position on the same particular axis. In a Bland-Altman plot, the mean difference in position (or bias) and 95% confidence limits of agreement are also calculated and visualized in the plot using Equation 2.

$$LoA = \chi_{obs.dif} \pm 1.96 * (\sigma_{obs.dif}) \quad (2)$$

where LoA is the limits of agreement
 $\chi_{obs.dif}$ is the mean observed difference in X or Y position
 $\sigma_{obs.dif}$ is the standard deviation of the observed difference in X or Y position

We do note that the Bland-Altman plot does not have a uniform criterion for what is an acceptable level of agreement because it depends on the variable being measured (Ranganathan & Aggarwal, 2017), but its limits and visualization provide us with a graphical representation of the bias and variance in position between the two methods. Furthermore, it can also help us point out how many outliers there are between the two methodologies. For our purposes, if we had found the data to have a difference in the limits of agreement above 100 meters, we would deem the two methods to have an insufficient or negative agreement as the variance would be too high, otherwise, we would deem the two methods to have a sufficient or positive agreement. Either way, all assessment methods are to be interpreted altogether accordingly before drawing complete conclusions regarding the connection between the two methodologies.

2.4.5 XY Position Difference Plots

To further analyze the deviations between the two methodologies, we employed Position Difference Plots. These plots were generated by calculating the positional differences along each axis between the remote sensing pixel locations (used

as the reference or minuend) and the particle positions from the Particle Tracking Model (PTM). Two aggregated plots were produced, combining data from all timestamps: one for the PTM approach that uses remotely sensed data as input, and another for the conventional approach that uses assumed sources such as tributaries or river mouths. These plots help reveal spatial patterns in the discrepancies between the two methodologies. Visually, the resulting plots resemble a dartboard, illustrating the spread and concentration of positional differences and providing insight into the spatial agreement or divergence of results.

3. Results and Discussion

3.1 Marine Litter Remote Sensing Findings

Remote sensing using spectral unmixing demonstrated the capability to differentiate marine debris from most other surface classes in the Manila Bay area, although confusion remained between debris and ships or vessels due to spectral similarities. Pixels with marine litter abundance greater than 50% were relatively rare, representing less than 10% of all pixels with any detected debris (>0% abundance). A sample image of detected marine litter points, demonstrating this sparseness, is shown in Figure 8. This indicates that while high-abundance debris is limited in spatial extent, lower-abundance classifications still provide meaningful information on the presence and spread of marine litter.

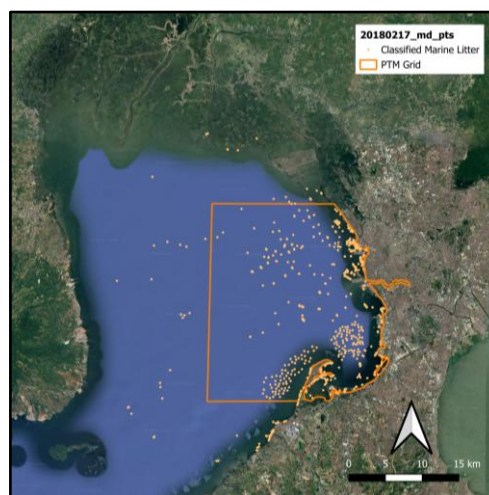


Figure 8. Sample classified marine litter (20180217)

Seasonal trends were evident in the classified point counts. Marine litter concentrations were generally higher during the dry season, while the wet season showed relatively lower detection rates. This fluctuation may be influenced by hydrological and meteorological factors such as increased rainfall and river discharge during wet months, which can disperse litter more widely or submerge it, reducing detection accuracy. In contrast, the dry season's calmer conditions may favor the accumulation and visibility of floating debris.

The classification accuracy of marine litter detection varied across the study period, with results ranging from 50% to 82%, and an overall accuracy of 68%. Notably, higher accuracies were achieved during the dry months, while lower accuracies were observed during the wet season. This seasonal difference may be attributed to changes in surface reflectance caused by water turbidity or wave conditions. Furthermore, several classified debris points were located near ICC cleanup sites as seen in Figure 9, lending further support to the method's effectiveness in

detecting real-world accumulation zones. These findings highlight the potential of remote sensing for operational monitoring of marine litter, although improvements are still needed for year-round consistency.



Figure 9. ICC field data maps for 2017 and 2018. Red circles indicate coinciding marine litter.

3.2 Particle Tracking Model Findings

The hydrodynamic model of the Manila Bay Pasig River outfall was developed using Delft3D-FLOW based on the specified boundary conditions and inputs detailed in the methodology. The simulation results, which included water level fluctuations and current vectors, were compared against current vector diagrams from Project E-SMART's 2021 Manila Bay dataset. This comparison confirmed that the model accurately reflected near-surface velocity directions during both ebb and flood tides. These findings were consistent with Project E-SMART's characterization of estuarine circulation in Manila Bay, supporting the validity of the model's performance. The hydrodynamic model current vectors can be viewed in Figure 10, with an attached youtube link to the animation. The water level animation can be viewed in the following link: https://youtu.be/phbbO_ftUc?si=NI088UynD2EgzXRN

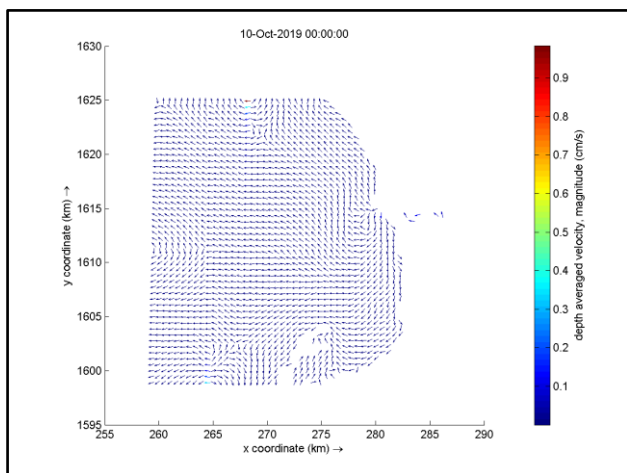


Figure 10. Hydrodynamic model current vectors (<https://youtu.be/DuuZdGBtw-s?si=chrF5KSjASi88Hr0>)

Using the hydrodynamic output, a particle-tracking simulation was performed in Delft3D-PART, where 188 marine litter particles were introduced from seven instantaneous release points on 14 March 2017. As described in the methodology, the release clusters were characterized by location, number of particles, and assigned plastic mass per particle. Particle dispersion and accumulation patterns were assessed for both dry and wet seasons from 2017 to 2019. During the dry season, particles tended to migrate and settle toward the northern portions of the domain,

with consistent accumulation near the Manila Bay Port area. In the wet season, marine litter tend to disperse, but with even greater accumulation observed in the Manila Bay Port area, along with additional buildup around the Cavite Spit. Each particle's track can be viewed in Figure 11, while the overall particle simulation can be viewed in the following youtube link: <https://youtu.be/NW1YiAKxcqQ?si=ixbMW-NoZPtKkKf5>

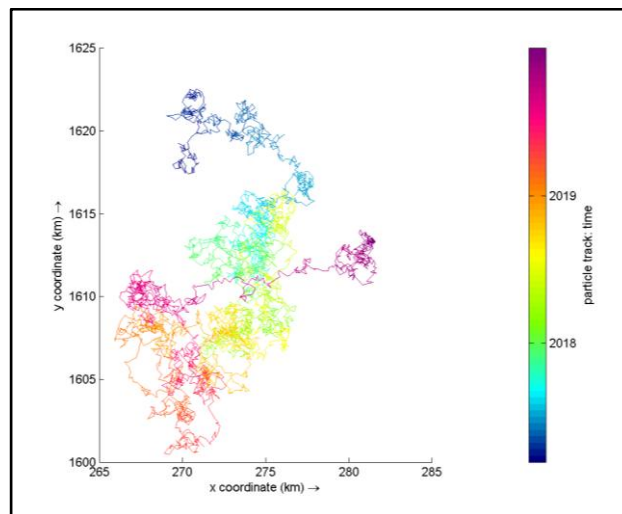


Figure 11. Particle tracking model particle tracks (<https://youtu.be/s8dhfN9YckA?si=KmUlwrFMTHQ1bsOS>)

Some particles exited the model boundaries over time, which prompted the tracking of particle counts at different dates corresponding to the availability of classified remote sensing imagery. A graph of the particle count over time indicated a steady decline, suggesting that full clearance of particles from the domain may take more than 30 years or result in persistent circulation within the system, as seen in Figure 12.

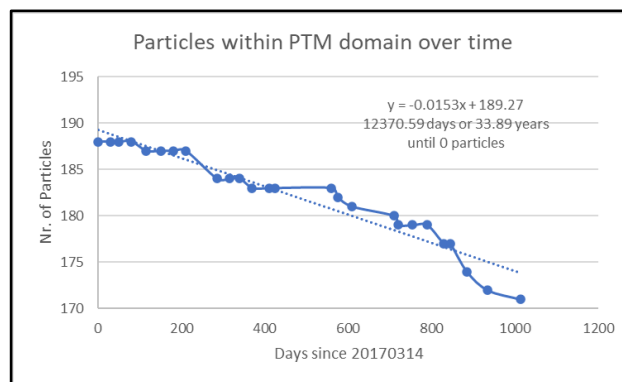


Figure 12. Particles within PTM domain over time for remote sensing inputs

As mentioned in the methodology, a control simulation was conducted using a single point release at the mouth of the Pasig River. This setup maintained the same number of particles and total plastic mass but used a reduced release radius to ensure all particles entered the waterway. Throughout the simulation, none of the particles exited the domain, instead remaining in circulation. This run showed that particles released from the river predominantly accumulated near the Manila Bay Port area. A similar pattern was seen in simulations using remotely sensed input sources. However, the incorporation of remotely sensed data allowed for a more comprehensive identification of accumulation zones throughout the model domain. This demonstrated the added value of integrating observational data

into modeling efforts for improved spatial coverage of marine litter detection. In replication, we suggest to also use GPS-tracked drifters and field or drone surveys to further bolster the validation at various spots within the model domain.

3.3 Spatial Distribution Assessment

The spatial distribution analysis, assessed using pixel-particle pair proximity maps, showed that remote sensing-based simulations aligned more closely with marine litter accumulations near the Manila Bay Port Area. In contrast, the control simulation using riverine sources mainly indicated concentrations near the same port area. However, the remote sensing approach identified a broader spatial spread of matched pairs, with litter accumulations also appearing in offshore and open water areas, as shown in the comparison in Figure 13. This suggests that marine litter distribution may be wider than what traditional riverine-source models can capture.

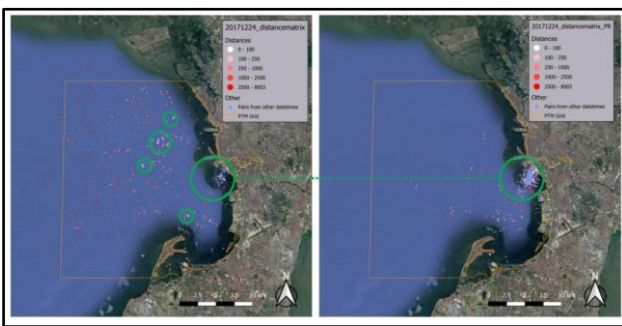


Figure 13. 20171224 Proximity Maps for RS source (left) and Riverine Source (right), with matched marine litter accumulations annotated

Nearest-point distance histograms were used to understand the positional differences between remote sensing classifications and PTM outputs. Results showed that most matched pairs were found within a few hundred meters of each other. While the remote sensing simulations had slightly larger average and median distances compared to the control, both methods had similar standard deviations, as seen in Figure 14 and 15. This indicates that even though remote sensing covered a broader area, the variation in positional accuracy was consistent with the riverine-based simulation.

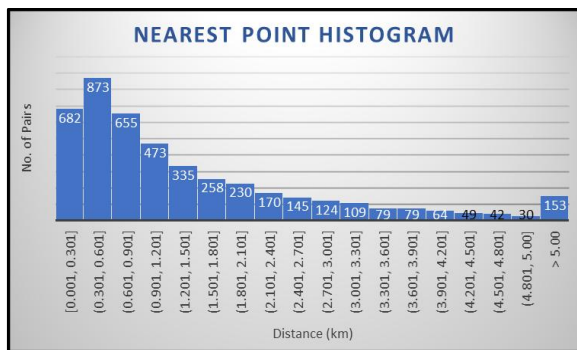


Figure 14. Nearest point histogram for remote sensing source

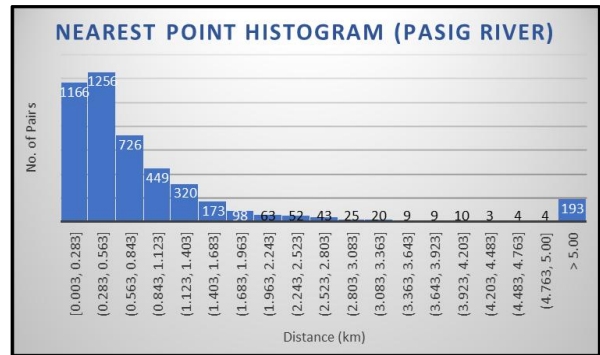


Figure 15. Nearest point histogram for remote sensing source

XY Equal Line Plots and Bland-Altman Plots were used to further assess spatial agreement between the two approaches. The equal line plots showed stronger linear correlations in the remote sensing-based simulations as shown in the summary in Table 2, indicating better overall alignment with observed data. Bland-Altman plots, however, revealed large differences in positional estimates for both methods, averaging around 5 kilometers in both axes for remote sensing sources, which shows a negative level of agreement between remote sensing and particle tracking models and high variance in position. However, in tandem with the high correlation equal line plot results, we note that there is likely a constant variance between the two methodologies caused by missing or unoptimized parameters. We hypothesize that this contradiction of between analyses is likely systematic, and can be optimized with the inclusion of more parameters, such as wind or beaching behavior, and high quality data like aerial photographs with higher resolution. The XY position difference plots in Figure 15 further confirmed this consistency in variance, suggesting that remote sensing inputs contribute to a more stable and spatially reliable representation of marine litter in hydrodynamic modeling.

Source	Average R2		Average R2 (after 6 months initialization)	
	X	Y	X	Y
Riverine	0.91	0.92	0.95	0.93
Remote Sensing	0.96	0.95	0.96	0.95

Table 2. XY equal line plot summary

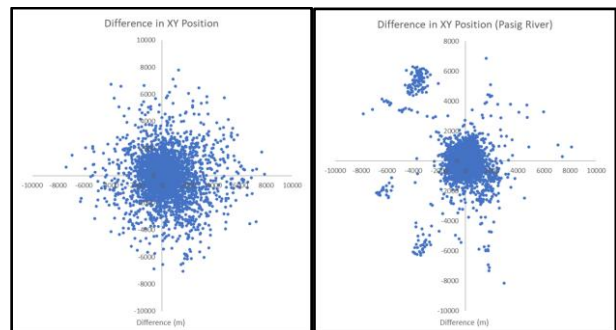


Figure 15. XY position difference plot for remote sensing source positions (left) and riverine source positions (right)

4. Conclusions

Between 2017 and 2019, we identified marine litter accumulation in the Manila Bay Pasig River Outfall using a combined approach

of remote sensing and particle tracking models, all powered by open-source tools such as Sentinel-2, SNAP, Delft3D-4, and QGIS. Remote sensing detected marine litter in both coastal and open waters, with results validated through image interpretation and ICC field data. These detections were then used as source points for particle tracking simulations, which were compared against a control simulation based on riverine input from the Pasig River. Both approaches pointed to the Manila Bay Port Area as a key accumulation zone, but the remote sensing-based simulation revealed a broader and more consistent spatial distribution. Based on the hydrodynamics, we hypothesize that plastic may accumulate on the surface due to the deeper bathymetry and coastline protrusions found near the port.

By analyzing the agreement between the two methods, we found strong correlations in their spatial outputs, with R^2 values above 0.90. However, positional differences averaging around 5 kilometers indicated that further refinement is needed. These findings highlight the potential of combining remote sensing and particle tracking to improve the accuracy of marine litter mapping and to inform practical applications such as targeted cleanup and water quality management. Table 3 summarizes the conclusions we identified regarding the two methodologies' advantages and disadvantages separately and in combination.

Conclusion for locating marine litter	Remote Sensing	Particle Tracking Models	Remote Sensing and Particle Tracking Models
Advantages	Wide spatial coverage, Direct locations of detected marine litter	High temporal coverage dependent on simulation timestep, adaptable to different local hydrodynamics	High spatial and temporal resolution, with potential to locate and verify marine litter in open waters, reproducible methodology
Disadvantages	Varied temporal coverage due to cloudy data and platform restrictions	Without high quality data and inputs, many assumptions potentially lead to miscalculated outliers or overestimated locations	Current technologies are not easily integrated with one another, requiring many technical limitations to be bypassed through assumptions

Table 3. Conclusions Summary

Based on these results, we recommend for the Manila Department of Public Service (DPS) and Manila Bay Coordinating Office (DENR-MBCO) to prioritize cleanup in the Manila Bay Port Area, while also extending efforts to nearby zones like the Cavite Spit and the northern coast, particularly during the wet season when plastic accumulation is highest. To enhance model accuracy, future studies should explore more focused study areas, integrate advanced detection methods such as deep learning (e.g., MariNeXt), and use higher spatial and temporal resolution data sources. Incorporating additional physical processes and accounting for changes such as coastal reclamation in hydrodynamic models will also make simulations

more realistic. Ultimately, we suggest developing an integrated system that merges remote sensing and modeling techniques to create a more consistent, accurate, and scalable framework for marine litter monitoring and management.

References

- Carlson, D. F., Suaria, G., Aliani, S., Fredj, E., Fortibuoni, T., Griffa, A., Russo, A., & Melli, V., 2017: Combining litter observations with a regional ocean model to identify sources and sinks of floating debris in a semi-enclosed basin: The Adriatic Sea. *Frontiers in Marine Science*, 4. <https://doi.org/10.3389/fmars.2017.00078>
- Cruz, L. L., & Shimozono, T., 2021: Transport of floating litter within Manila Bay, Philippines. *Marine Pollution Bulletin*, 163, 111944. <https://doi.org/10.1016/j.marpolbul.2020.111944>
- Danilov, A., & Serdiukova, E., 2024: Review of Methods for Automatic Plastic Detection in Water Areas Using Satellite Images and Machine Learning. *Sensors*, 24(16), 5089–5089. <https://doi.org/10.3390/s24165089>
- ESRI., n.d. Point Distance (Analysis)—ArcGIS Pro | Documentation. Pro.arcgis.com. <https://pro.arcgis.com/en/pro-app/latest/tool-reference/analysis/point-distance.htm> (7 June 2025).
- Kikaki, K., Kakogeorgiou, I., Hoteit, I., & Karantzalos, K., 2024: Detecting Marine pollutants and Sea Surface features with Deep learning in Sentinel-2 imagery. *ISPRS Journal of Photogrammetry and Remote Sensing*, 210, 39–54. <https://doi.org/10.1016/j.isprsjprs.2024.02.017>
- Meijer, L. J. J., van Emmerik, T., van der Ent, R., Schmidt, C., & Lebreton, L., 2021: More than 1000 rivers account for 80% of global riverine plastic emissions into the ocean. *Science Advances*, 7(18). <https://doi.org/10.1126/sciadv.aaz5803>
- Paler, M. K. O., Tabañag, I. D. F., Siacor, F. D. C., Geraldino, P. J. L., Walton, M. E. M., Dunn, C., Skov, M. W., Hiddink, J. G., & Taboada, E. B., 2022: Elucidating the surface macroplastic load, types and distribution in mangrove areas around Cebu Island, Philippines and its policy implications. *Science of the Total Environment*, 838, 156408. <https://doi.org/10.1016/j.scitotenv.2022.156408>
- Politikos, D. V., Ioakeimidis, C., Papatheodorou, G., & Tsiaras, K., 2017: Modeling the fate and distribution of floating litter particles in the Aegean Sea (E. Mediterranean). *Frontiers in Marine Science*, 4. <https://doi.org/10.3389/fmars.2017.00191>
- Ranganathan, P., Pramesh, C., & Aggarwal, R., 2017: Common pitfalls in statistical analysis: Measures of agreement. *Perspectives in Clinical Research*, 8(4), 187. https://doi.org/10.4103/picr.picr_123_17
- Waqas, M., Wong, M. S., Stocchino, A., Abbas, S., Hafeez, S., & Zhu, R., 2023: Marine plastic pollution detection and identification by using remote sensing-meta analysis. *Marine Pollution Bulletin*, 197, 115746. <https://doi.org/10.1016/j.marpolbul.2023.115746>
- Zambianchi, E., Trani, M., & Falco, P., 2017: Lagrangian Transport of Marine Litter in the Mediterranean Sea. *Frontiers in Environmental Science*, 5. <https://doi.org/10.3389/fenvs.2017.00005>